

Bound States of a Minimally Interacting Spin-0 and Spin-1/2 Constituent in the Instantaneous Approximation

G. Bruce Mainland

Department of Physics
The Ohio State University
Columbus, OH 43210, USA

Abstract

Bound-state solutions are obtained numerically in the instantaneous approximation for a spin-0 and spin-1/2 constituent that interact via minimal electrodynamics. To solve the integral equations in momentum space, a method is developed for integrating over the logarithmic singularity in kernels, making it possible to use basis functions that essentially automatically satisfy the boundary conditions. For bound-state solutions that decrease rapidly at small and large values of momentum, accurate solutions are obtained with significantly fewer basis functions when the solution is expanded in terms of these more general basis functions. The presence of a derivative coupling in single-photon exchange complicates the construction of the Bethe-Salpeter equation in the instantaneous approximation and, in the non-relativistic limit, gives rise to an additional electrostatic potential term that is second order in the coupling constant and decreases as the square of the distance between constituents.

PACS numbers: 02.60.-x, 03.65.Pm, 11.10.St

1 Introduction

There has been a growing interest in solving relativistic, bound-state equations both because important bound-state systems are relativistic and because the development of high-speed computers makes it possible to solve such equations. The Bethe-Salpeter equation [1], which is based on field theory, is covariant and reduces to the Schrödinger equation in the nonrelativistic limit, is the appropriate equation to use in describing relativistic bound states. Unfortunately, even numerically the two-body bound-state equation is exceedingly difficult to solve [2]. For this reason various approximations such as the Blankenbecler-Sugar approximation [3] or the instantaneous approximation[1,4] are often made that reduce the covariant equation in four dimensions to an approximately-covariant equation in three dimensions. In this article attention is restricted to the instantaneous approximation although the general methods developed here can be used in the implementation of other approximation schemes that reduce the Bethe-Salpeter equation to a three-dimensional equation.

The instantaneous approximation, which is the approximation that the binding quanta travel instantaneously between the bound constituents, was first introduced in the original article by Bethe and Salpeter [1] and was used in their calculation to demonstrate that the Schrödinger equation is the nonrelativistic limit of the Bethe-Salpeter equation. More in the spirit of this work, Salpeter [4] made the instantaneous approximation to reduce the Bethe-Salpeter equation to a three-dimensional equation and calculated corrections to the fine structure of hydrogen-like atoms. The presence of a derivative coupling in single-photon exchange complicates the construction of the Bethe-Salpeter equation in the instantaneous approximation and, in addition to terms that are first order in the coupling constant, gives rise to two terms that are second order. The “seagull” interaction yields the same two second-order interactions, but with different strengths. In the nonrelativistic limit, the second-order interaction becomes an electrostatic potential term that decreases as the square of the distance between the constituents.

A major difficulty in solving equations numerically when the instantaneous approximation is made arises because a logarithmic singularity occurs in the kernel of the integral equations. Gammel and Menzel [5] overcome the problem by using a special weighting scheme in the neighborhood of the singularity, and Eyre and Vary [6] introduce a numerical cutoff and then correct

for the effects of the cutoff using perturbation theory. Later Spence and Vary [7] use B-splines [8] as basis functions and perform all integrals analytically. Since the B-splines are polynomials, their method is restricted to polynomial basis functions. In this article a method is used to integrate over the logarithmic singularity that allows the use of more general basis functions that essentially automatically satisfy the boundary conditions and are not necessarily polynomials. This new method, which is very simple conceptually, is a generalization of the method introduced in Ref. 7. For bound states that decrease rapidly at small and large values of momentum, accurate solutions are obtained with significantly fewer basis functions when these more general basis functions are used.

Two physical problems that are of immediate interest are constituent models of quarks and leptons [9,10] and constituent-quark models of mesons [11]. Equations that account for some relativistic effects have had success in describing the properties of both light and heavy mesons [11]. The fact that there are three families of leptons, much as there are families of elements or families of hadrons, suggests that the leptons might be composite. The discovery of neutrino oscillations [12] raises the possibility that neutrinos might also be composite [13]. If the electron, muon and tau are bound states of a single system, the system is necessarily relativistic: The mass of the tau must, of course, be less than the sum of the masses of the bound, constituent particles. Since the ratio of the electron's mass to that of the tau's equals 1/3536, the mass of the electron is less than 1/3536 of the sum of the constituent masses, indicating highly relativistic binding.

The Bethe-Salpeter equation discussed here has been solved exactly in the strong binding (zero energy) limit when the ladder approximation is made [10]. In the instantaneous approximation the numerical solutions obtained here are not in good agreement with the exact zero-energy solutions so, not surprisingly, the instantaneous approximation is not satisfactory for very strongly bound states.

To estimate the accuracy of each solution, in the physical region the left- and right-hand sides of the equation are calculated midway between each knot, and a reliability coefficient R [14], which is a statistical measure of how accurately the left- and right-hand sides agree at the selected points, is calculated. Examining points where the left- and right-hand sides of the equation agree least well reveals possible problems with solutions and suggests possible remedies.

2 Derivation and Separation of the Bethe–Salpeter Equation in the Instantaneous Approximation

When a spin-0 field $\phi(x)$, which represents a quanta with charge Q and mass M , interacts via minimal electrodynamics with a spin-1/2 field $\Psi(x)$, which represents a quanta with charge q and mass m , the renormalizable Lagrangian is [15]

$$L =: [(\imath\partial^\mu - QA^\mu)\phi][(-\imath\partial_\mu - QA_\mu)\phi^+] - M^2\phi^+\phi + \bar{\Psi}\gamma_\mu(\imath\partial^\mu - qA^\mu)\Psi - m\bar{\Psi}\Psi - \frac{1}{4}F_{\mu\nu}F^{\mu\nu} : \quad (2.1)$$

where $F_{\mu\nu} = \partial_\nu A_\mu - \partial_\mu A_\nu$.

The two-particle, Bethe-Salpeter wave function is defined by

$$\chi_K(x_1, x_2) = < 0 | T(\Psi(x_1)\phi(x_2)) | K > . \quad (2.2)$$

In (2.2) the symbol T represents time ordering and the letter K labels the four-momentum of the bound state. The center-of-mass coordinates X^μ are defined by

$$X^\mu = \xi x_1^\mu + (1 - \xi)x_2^\mu, \quad (2.3)$$

and the relative coordinates x^μ by

$$x^\mu = x_1^\mu - x_2^\mu. \quad (2.4)$$

When the parameter ξ is given by $\xi = m/(m + M)$, the usual nonrelativistic definition of center-of-mass coordinates results. As will be seen, the parameter ξ drops out of the Bethe-Salpeter equation when the instantaneous approximation is made so there is no need to make a specific choice. The dependence of $\chi_K(x_1, x_2)$ on the center-of-mass coordinates factors with the result that $\chi_K(x_1, x_2)$ can be rewritten as

$$\chi_K(x_1, x_2) = (2\pi)^{-3/2}e^{-iX^\mu K_\mu}\chi_K(x). \quad (2.5)$$

Denoting the Fourier transform of $\chi_K(x)$ by $\chi_K(p)$, the Bethe-Salpeter equation is

$$\begin{aligned}
& (p^\mu \gamma_\mu + \xi K^\mu \gamma_\mu - m) \{ [p^\mu - (1 - \xi) K^\mu] [p_\mu - (1 - \xi) K_\mu] - M^2 \} \chi_K(p) \\
&= \frac{i q Q}{(2\pi)^4} \int_{-\infty}^{\infty} \frac{d^4 q}{(p - q)^2 + i\epsilon} [p^\mu \gamma_\mu + q^\mu \gamma_\mu - 2(1 - \xi) K^\mu \gamma_\mu] \chi_K(q) \\
&+ \frac{4(qQ)^2}{(2\pi)^8} \int_{-\infty}^{\infty} \frac{d^4 q}{q^2 - m^2 + i\epsilon} \frac{2m - q^\mu \gamma_\mu}{(p - q + \xi K)^2 + i\epsilon} \times \\
&\quad \int_{-\infty}^{\infty} \frac{d^4 k}{(q - k - \xi K)^2 + i\epsilon} \chi_K(k). \tag{2.6}
\end{aligned}$$

A charged, spin-0 boson interacts electromagnetically through two fundamentally different processes: single-photon exchange and the “seagull” interaction. In the above equation the terms proportional to qQ and $(qQ)^2$ arise, respectively, from these two interactions. Although the “seagull” interaction is second order in the coupling constant, it has been included in the Bethe-Salpeter equation to determine its effect on solutions. The spirit of this calculation, then, is similar to others dealing with the Bethe-Salpeter equation whereby the ladder approximation is made, but some solutions with large coupling constants are studied. The Feynman diagrams for these two interactions are shown in Fig. 2.1

The instantaneous approximation [1,4] is made by making the replacement

$$\frac{1}{k^2 + i\epsilon} = \frac{1}{k_0^2 - \mathbf{k}^2 + i\epsilon} \rightarrow \frac{1}{-\mathbf{k}^2 + i\epsilon} \tag{2.7}$$

in each of the three photon propagators in (2.6). Defining

$$\Psi_K(\mathbf{k}) \equiv \int_{-\infty}^{\infty} dk_0 \chi_K(k), \tag{2.8a}$$

and

$$\phi_K(\mathbf{k}) \equiv \int_{-\infty}^{\infty} dk_0 k_0 \chi_K(k), \tag{2.8b}$$

the integral over q_0 in the single-photon-exchange term in (2.6) and the integral over k_0 in the “seagull” term can be carried out immediately. In the

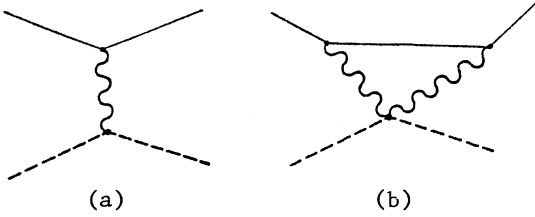


Figure 2.1: Feynman diagrams for (a) single-photon exchange and (b) the “seagull” interaction. The solid, dashed and wavy lines represent a spin-1/2 fermion, a spin-0 boson and a photon, respectively.

“seagull” term it is then possible to integrate over q_0 . Going to the center-of-mass frame where $K^\mu = (E, 0)$, (2.6) becomes

$$\begin{aligned}
 & [p^0\gamma^0 - p^i\gamma^i + \xi E\gamma_0 - m]\{[p^0 - (1 - \xi)E]^2 - p^i p^i - M^2\}\chi_E(p) \\
 &= -\frac{iqQ}{(2\pi)^4} \int_{-\infty}^{\infty} \frac{d^3 q}{(\mathbf{p} - \mathbf{q})^2} [\gamma^0 p^0 - \gamma^i(p^i + q^i) - 2(1 - \xi)E\gamma^0] \Psi_E(\mathbf{q}) \\
 &\quad - \frac{iqQ}{(2\pi)^4} \int_{-\infty}^{\infty} \frac{d^3 q}{(\mathbf{p} - \mathbf{q})^2} \gamma^0 \phi_E(\mathbf{q}) \\
 &\quad - \frac{2i(qQ)^2}{(2\pi)^7} \int_{-\infty}^{\infty} \frac{d^3 q}{(\mathbf{p} - \mathbf{q})^2} \frac{2m + \gamma^i q^i}{\omega_m(q)} \int_{-\infty}^{\infty} \frac{d^3 k}{(\mathbf{q} - \mathbf{k})^2} \Psi_E(\mathbf{k}). \tag{2.9}
 \end{aligned}$$

In the above equation $\chi_E(p)$ is the value of $\chi_K(p)$ in the center-of-mass frame, etc., and $\omega_m(q) \equiv (m^2 + q^2)^{1/2}$.

Solving (2.9) for $\chi_E(p)$, integrating over p^0 on both sides of the equation and using (2.8) yields

$$\omega_M(p)E\Psi_E(\mathbf{p}) = \frac{\omega_M(p)}{\omega_m(p)} [\omega_M(p) + \omega_m(p)][\gamma^0\gamma^i p^i + \gamma^0 m] \Psi_E(\mathbf{p})$$

$$\begin{aligned}
& + \frac{qQ}{16\pi^3} \int_{-\infty}^{\infty} \frac{d^3q}{(\mathbf{p} - \mathbf{q})^2} \left\{ (1 - \xi)E + \left[\frac{\omega_M(p) + \omega_m(p)}{\omega_m(p)} \right] \gamma^0 \gamma^i p^i \right. \\
& \quad \left. + \frac{\omega_M(p)}{\omega_m(p)} \gamma^0 m + \gamma^0 \gamma^i q^i \right\} \Psi_E(\mathbf{q}) \\
& - \frac{Qq}{16\pi^3} \int_{-\infty}^{\infty} \frac{d^3q}{(\mathbf{p} - \mathbf{q})^2} \phi_E(\mathbf{q}) \\
& - \frac{(qQ)^2}{(2\pi)^6} \int_{-\infty}^{\infty} \frac{d^3q}{(\mathbf{p} - \mathbf{q})^2} \frac{2m\gamma^0 + \gamma^0 \gamma^i q^i}{\omega_m(q)} \int_{-\infty}^{\infty} \frac{d^3k}{(\mathbf{q} - \mathbf{k})^2} \Psi_E(\mathbf{k}). \quad (2.10)
\end{aligned}$$

Eq. (2.10) cannot readily be solved because of the presence of the two functions Ψ_E and ϕ_E that are related as indicated in (2.8). The function ϕ_E is present, of course, as a consequence of the derivative coupling.

It is possible, however, to express ϕ_E in terms of Ψ_E as follows: By dividing both sides of (2.9) by $\{[p^0 - (1 - \xi)E]^2 - p^i p^i - M^2\}$ and then integrating over p^0 , a second equation is obtained that involves both Ψ_E and ϕ_E :

$$\begin{aligned}
& \omega_M(p)\phi_E(\mathbf{p}) = \omega_M(p) (-\xi E + \gamma^0 \gamma^i p^i + \gamma^0 m) \Psi_E(\mathbf{p}) \\
& + \frac{qQ}{16\pi^3} \int_{-\infty}^{\infty} \frac{d^3q}{(\mathbf{p} - \mathbf{q})^2} [(1 - \xi)E + \gamma^0 \gamma^i (p^i + q^i)] \Psi_E(\mathbf{q}) \\
& - \frac{qQ}{16\pi^3} \int_{-\infty}^{\infty} \frac{d^3q}{(\mathbf{p} - \mathbf{q})^2} \phi_E(\mathbf{q}) \\
& - \frac{(qQ)^2}{(2\pi)^6} \int_{-\infty}^{\infty} \frac{d^3q}{(\mathbf{p} - \mathbf{q})^2} \frac{2m\gamma^0 + \gamma^0 \gamma^i q^i}{\omega_m(q)} \int_{-\infty}^{\infty} \frac{d^3k}{(\mathbf{q} - \mathbf{k})^2} \Psi_E(\mathbf{k}) \quad (2.11)
\end{aligned}$$

Subtracting (2.11) from (2.10) and solving for $\phi_E(\mathbf{p})$ yields

$$\phi_E(\mathbf{p}) = (1 - \xi)E\Psi_E(\mathbf{p})$$

$$-\frac{1}{\omega_m(p)} (\gamma^0 \gamma^i p^i + \gamma^0 m) [\omega_M(p) \Psi_E(\mathbf{p}) + \frac{qQ}{16\pi^3} \int_{-\infty}^{\infty} \frac{d^3 q}{(\mathbf{p} - \mathbf{q})^2} \Psi_E(\mathbf{q})]. \quad (2.12)$$

Using (2.12) to express $\phi_E(\mathbf{p})$ in terms of Ψ_E , (2.10) becomes the Bethe-Salpeter equation in the instantaneous approximation:

$$\begin{aligned} \omega_M(p) E \Psi_E(\mathbf{p}) &= \frac{\omega_M(p)}{\omega_m(p)} [\omega_M(p) + \omega_m(p)] [\gamma^0 \gamma^i p^i + \gamma^0 m] E \Psi_E(\mathbf{p}) \\ &+ \frac{qQ}{16\pi^3} \int_{-\infty}^{\infty} \frac{d^3 q}{(\mathbf{p} - \mathbf{q})^2} \left\{ \left[\frac{\omega_M(p)}{\omega_m(p)} + 1 \right] \gamma^0 \gamma^i p^i + \left[\frac{\omega_M(q)}{\omega_m(q)} + 1 \right] \gamma^0 \gamma^i q^i \right. \\ &\quad \left. + \left[\frac{\omega_M(p)}{\omega_m(p)} + \frac{\omega_M(q)}{\omega_m(q)} \right] \gamma^0 m \right\} \Psi_E(\mathbf{q}) \\ &+ \frac{(qQ)^2}{4(2\pi)^6} \int_{-\infty}^{\infty} \frac{d^3 q}{(\mathbf{p} - \mathbf{q})^2} \frac{m \gamma^0 + \gamma^0 \gamma^i q^i}{\omega_m(q)} \int_{-\infty}^{\infty} \frac{d^3 k}{(\mathbf{q} - \mathbf{k})^2} \Psi_E(\mathbf{k}) \\ &- \frac{(qQ)^2}{(2\pi)^6} \int_{-\infty}^{\infty} \frac{d^3 q}{(\mathbf{p} - \mathbf{q})^2} \frac{2m \gamma^0 + \gamma^0 \gamma^i q^i}{\omega_m(q)} \int_{-\infty}^{\infty} \frac{d^3 k}{(\mathbf{q} - \mathbf{k})^2} \Psi_E(\mathbf{k}) \quad (2.13) \end{aligned}$$

In (2.13) the final two terms, which are proportional to $(qQ)^2$, arise from the derivative coupling in single photon exchange and the “seagull” interaction, respectively.

Eq. (2.13) is much easier to solve numerically than the Bethe-Salpeter equation, primarily because it is much easier to obtain solutions with real energy eigenvalues. Specifically, equations of the form (2.13) can be solved numerically by converting them to matrix eigenvalue equations. When each side is multiplied by $\Psi_E^\dagger(\mathbf{p})$ and integrated over $d^3 p$, excluding the eigenvalue E , the quantity on the left-hand side is Hermitian and positive definite and the quantity on the right-hand side is Hermitian. As a consequence the energy eigenvalue must be real [16]. The Hermiticity results from the fact that the momenta \mathbf{p} and \mathbf{q} appear symmetrically on the right-hand side of (2.13). In the very special cases where the Bethe-Salpeter equation possesses the Hermiticity properties of (2.13), the equation is relatively easy to solve numerically [2,17] in spite of the fact that after separation of the two angular variables, it is still an integral or partial differential equation in two variables.

Solutions to (2.13) are of the form

$$\Psi_E(\mathbf{p}) = \begin{bmatrix} G^{(\pm)}(p)\phi^{(\pm)}(\theta, \varphi) \\ F^{(\pm)}(p)\phi^{(\mp)}(\theta, \varphi) \end{bmatrix}, \quad (2.14)$$

where the $\phi^{(\pm)}(\theta, \varphi)$ are the same functions [15] that represent the angular dependence of the bound-state solutions to the Dirac equation when the potential is spherically symmetric. After the angular integration is performed using Hecke's theorem [18,19,20,10], the angular variables separate. Multiplying the resulting upper and lower equations by p and $-p$, respectively, yields

$$\begin{aligned} E\omega_M(p) & \begin{bmatrix} pG^{(\pm)}(p) \\ pF^{(\pm)}(p) \end{bmatrix} \\ &= \frac{\omega_M(p)}{\omega_m(p)} [\omega_M(p) + \omega_m(p)] \left\{ p \begin{bmatrix} pF^{(\pm)}(p) \\ pG^{(\pm)}(p) \end{bmatrix} + m \begin{bmatrix} pG^{(\pm)}(p) \\ -pF^{(\pm)}(p) \end{bmatrix} \right\} \\ &+ \frac{qQ}{8\pi^2} p \left[\frac{\omega_M(p)}{\omega_m(p)} + 1 \right] \begin{bmatrix} \int dq qF^{(\pm)}(q)Q_{j\pm\frac{1}{2}}\left(\frac{p^2+q^2}{2pq}\right) \\ \int dq qG^{(\pm)}(q)Q_{j\mp\frac{1}{2}}\left(\frac{p^2+q^2}{2pq}\right) \end{bmatrix} \\ &+ \frac{qQ}{8\pi^2} \int q dq \left[\frac{\omega_M(q)}{\omega_m(q)} + 1 \right] \begin{bmatrix} qF^{(\pm)}(q)Q_{j\mp\frac{1}{2}}\left(\frac{p^2+q^2}{2pq}\right) \\ qG^{(\pm)}(q)Q_{j\pm\frac{1}{2}}\left(\frac{p^2+q^2}{2pq}\right) \end{bmatrix} \\ &+ \frac{qQ}{8\pi^2} m \int dq \left[\frac{\omega_M(p)}{\omega_m(p)} + \frac{\omega_M(q)}{\omega_m(q)} \right] \begin{bmatrix} qG^{(\pm)}(q)Q_{j\mp\frac{1}{2}}\left(\frac{p^2+q^2}{2pq}\right) \\ -qF^{(\pm)}(q)Q_{j\pm\frac{1}{2}}\left(\frac{p^2+q^2}{2pq}\right) \end{bmatrix} \\ &+ \frac{q^2Q^2}{4(2\pi)^4} \int \frac{dq}{\omega_m(q)} \int dk \left\{ m \begin{bmatrix} kG^{(\pm)}(k)Q_{j\mp\frac{1}{2}}\left(\frac{k^2+q^2}{2kq}\right)Q_{j\mp\frac{1}{2}}\left(\frac{p^2+q^2}{2pq}\right) \\ -kF^{(\pm)}(k)Q_{j\pm\frac{1}{2}}\left(\frac{k^2+q^2}{2kq}\right)Q_{j\pm\frac{1}{2}}\left(\frac{p^2+q^2}{2pq}\right) \end{bmatrix} \right\} \end{aligned}$$

$$\begin{aligned}
& +q \left[\begin{array}{l} kF^{(\pm)}(k)Q_{j\pm\frac{1}{2}}\left(\frac{k^2+q^2}{2kq}\right)Q_{j\mp\frac{1}{2}}\left(\frac{p^2+q^2}{2pq}\right) \\ kG^{(\pm)}(k)Q_{j\mp\frac{1}{2}}\left(\frac{k^2+q^2}{2kq}\right)Q_{j\pm\frac{1}{2}}\left(\frac{p^2+q^2}{2pq}\right) \end{array} \right] \} \\
& -\frac{q^2Q^2}{(2\pi)^4} \int \frac{dq}{\omega_m(q)} \int dk \left\{ 2m \left[\begin{array}{l} kG^{(\pm)}(k)Q_{j\mp\frac{1}{2}}\left(\frac{k^2+q^2}{2kq}\right)Q_{j\mp\frac{1}{2}}\left(\frac{p^2+q^2}{2pq}\right) \\ -kF^{(\pm)}(k)Q_{j\pm\frac{1}{2}}\left(\frac{k^2+q^2}{2kq}\right)Q_{j\pm\frac{1}{2}}\left(\frac{p^2+q^2}{2pq}\right) \end{array} \right] \right. \\
& \left. +q \left[\begin{array}{l} kF^{(\pm)}(k)Q_{j\pm\frac{1}{2}}\left(\frac{k^2+q^2}{2kq}\right)Q_{j\mp\frac{1}{2}}\left(\frac{p^2+q^2}{2pq}\right) \\ kG^{(\pm)}(k)Q_{j\mp\frac{1}{2}}\left(\frac{k^2+q^2}{2kq}\right)Q_{j\pm\frac{1}{2}}\left(\frac{p^2+q^2}{2pq}\right) \end{array} \right] \right\}, \quad (2.15)
\end{aligned}$$

where $Q_{j\pm\frac{1}{2}}$ is a Legendre function of the second kind and

$$\omega_M(p) \equiv \sqrt{p^2 + M^2}, \quad \omega_m(p) \equiv \sqrt{p^2 + m^2}. \quad (2.16)$$

To rewrite (2.15) in terms of dimensionless variables, the two masses are first rewritten as follows:

$$m \equiv m_0(1 - \Delta), \quad M \equiv m_0(1 + \Delta). \quad (2.17)$$

The dimensionless momentum p' is defined by

$$p' \equiv \frac{p}{m_0}, \quad (2.18)$$

and the dimensionless energy ϵ by

$$\epsilon \equiv \frac{E}{M + m} = \frac{E}{2m_0}. \quad (2.19)$$

Defining

$$\omega_+(p') \equiv \frac{\omega_M(p)}{m_0} = \sqrt{(1 + \Delta)^2 + p'^2}, \quad (2.20a)$$

and

$$\omega_-(p') \equiv \frac{\omega_m(p)}{m_0} = \sqrt{(1 - \Delta)^2 + p'^2}, \quad (2.20b)$$

and omitting primes since all variables are now dimensionless, (2.15) becomes

$$\begin{aligned}
& 2\epsilon\omega_+(p) \begin{bmatrix} pG^{(\pm)}(p) \\ pF^{(\pm)}(p) \end{bmatrix} \\
&= \frac{\omega_+(p)}{\omega_-(p)} [\omega_+(p) + \omega_-(p)] \left\{ p \begin{bmatrix} pF^{(\pm)}(p) \\ pG^{(\pm)}(p) \end{bmatrix} + (1 - \Delta) \begin{bmatrix} pG^{(\pm)}(p) \\ -pF^{(\pm)}(p) \end{bmatrix} \right\} \\
&+ \frac{qQ}{8\pi^2} p \left[\frac{\omega_+(p)}{\omega_-(p)} + 1 \right] \int dq \begin{bmatrix} qF^{(\pm)}(q)Q_{j\pm\frac{1}{2}}\left(\frac{p^2+q^2}{2pq}\right) \\ qG^{(\pm)}(q)Q_{j\mp\frac{1}{2}}\left(\frac{p^2+q^2}{2pq}\right) \end{bmatrix} \\
&+ \frac{qQ}{8\pi^2} \int q dq \left[\frac{\omega_+(q)}{\omega_-(q)} + 1 \right] \begin{bmatrix} qF^{(\pm)}(q)Q_{j\mp\frac{1}{2}}\left(\frac{p^2+q^2}{2pq}\right) \\ qG^{(\pm)}(q)Q_{j\pm\frac{1}{2}}\left(\frac{p^2+q^2}{2pq}\right) \end{bmatrix} \\
&+ \frac{qQ}{8\pi^2} (1 - \Delta) \int dq \left[\frac{\omega_+(p)}{\omega_-(p)} + \frac{\omega_+(q)}{\omega_-(q)} \right] \begin{bmatrix} qG^{(\pm)}(q)Q_{j\mp\frac{1}{2}}\left(\frac{p^2+q^2}{2pq}\right) \\ -qF^{(\pm)}(q)Q_{j\pm\frac{1}{2}}\left(\frac{p^2+q^2}{2pq}\right) \end{bmatrix} \\
&+ \frac{(qQ)^2}{4(2\pi)^4} \int \frac{dq}{\omega_-(q)} \int dk \} (1 - \Delta) \begin{bmatrix} kG^{(\pm)}(k)Q_{j\mp\frac{1}{2}}\left(\frac{k^2+q^2}{2kq}\right)Q_{j\mp\frac{1}{2}}\left(\frac{p^2+q^2}{2pq}\right) \\ -kF^{(\pm)}(k)Q_{j\pm\frac{1}{2}}\left(\frac{k^2+q^2}{2kq}\right)Q_{j\pm\frac{1}{2}}\left(\frac{p^2+q^2}{2pq}\right) \end{bmatrix} \\
&+ q \left[\begin{bmatrix} kF^{(\pm)}(k)Q_{j\pm\frac{1}{2}}\left(\frac{k^2+q^2}{2kq}\right)Q_{j\mp\frac{1}{2}}\left(\frac{p^2+q^2}{2pq}\right) \\ kG^{(\pm)}(k)Q_{j\mp\frac{1}{2}}\left(\frac{k^2+q^2}{2kq}\right)Q_{j\pm\frac{1}{2}}\left(\frac{p^2+q^2}{2pq}\right) \end{bmatrix} \right\} \\
&- \frac{(qQ)^2}{(2\pi)^4} \int \frac{dq}{\omega_-(q)} \int dk \left\{ 2(1 - \Delta) \begin{bmatrix} kG^{(\pm)}(k)Q_{j\mp\frac{1}{2}}\left(\frac{k^2+q^2}{2kq}\right)Q_{j\mp\frac{1}{2}}\left(\frac{p^2+q^2}{2pq}\right) \\ -kF^{(\pm)}(k)Q_{j\pm\frac{1}{2}}\left(\frac{k^2+q^2}{2kq}\right)Q_{j\pm\frac{1}{2}}\left(\frac{p^2+q^2}{2pq}\right) \end{bmatrix} \right. \\
&\quad \left. + q \begin{bmatrix} kF^{(\pm)}(k)Q_{j\pm\frac{1}{2}}\left(\frac{k^2+q^2}{2kq}\right)Q_{j\mp\frac{1}{2}}\left(\frac{p^2+q^2}{2pq}\right) \\ kG^{(\pm)}(k)Q_{j\mp\frac{1}{2}}\left(\frac{k^2+q^2}{2kq}\right)Q_{j\pm\frac{1}{2}}\left(\frac{p^2+q^2}{2pq}\right) \end{bmatrix} \right\}. \tag{2.21}
\end{aligned}$$

The set of two equations with the top signs is transformed into the set of two equations with the bottom signs and vice versa with the following replacements:

$$G^{(+)} \leftrightarrow F^{(-)}, \quad F^{(+)} \leftrightarrow -G^{(-)}, \quad \epsilon \leftrightarrow -\epsilon \quad (2.22)$$

As a consequence only the equations for $F^{(+)}$ and $G^{(+)}$ need be solved. For notational convenience the superscripts on $F^{(+)}$ and $G^{(+)}$ are omitted in future equations.

3 Solutions to the Nonrelativistic Reduction of the Bethe-Salpeter Equation

In this section the nonrelativistic reduction of the Bethe-Salpeter equation, which is just the Schrödinger equation, is solved numerically in momentum space. Although the equation can be solved analytically, here it is solved numerically to illustrate techniques that will be used to solve the Bethe-Salpeter equation in the instantaneous approximation, an equation that, apparently, cannot in general be solved analytically. A method is introduced for handling the singularity in the kernel that makes possible the use of basis functions that automatically satisfy the boundary conditions both at small and large momenta. For angular momentum states $\ell = 0$ and $\ell = 1$, these basis functions are not an improvement over the basis functions used by Spence and Vary [7] that only automatically satisfy the boundary conditions for small momentum, but for angular momentum states $\ell > 1$, the basis functions used here converge to a solution much more efficiently.

Once the instantaneous approximation has been made, it is straightforward to make a nonrelativistic reduction [1]. Keeping the lowest order term in each of the two interaction terms, proportional to qQ and $(qQ)^2$, respectively,

$$\begin{aligned} E' \Psi(\mathbf{p}) &= \left(\frac{\mathbf{p}^2}{2M} + \frac{\mathbf{p}^2}{2m} \right) \Psi(\mathbf{p}) + \frac{qQ}{8\pi^3} \int_{-\infty}^{\infty} \frac{d^3 q}{(\mathbf{p} - \mathbf{q})^2} \Psi(\mathbf{q}) \\ &\quad + (1 - 8) \frac{(qQ)^2}{2^8 \pi^6 M} \int_{-\infty}^{\infty} \frac{d^3 q}{(\mathbf{p} - \mathbf{q})^2} \int_{-\infty}^{\infty} \frac{d^3 k}{(\mathbf{q} - \mathbf{k})^2} \Psi(\mathbf{k}). \end{aligned} \quad (3.1)$$

The nonrelativistic energy E' is related to the relativistic energy E by $E = m + M + E'$. In the final term in the above equation, the integer “1” in the

first parenthesis is from single-photon exchange while the integer “-8” is from the “seagull” interaction.

Fourier transforming (3.1),

$$\begin{aligned} E' \Psi(\mathbf{x}) = & -\left(\frac{1}{2M} + \frac{1}{2m}\right) \nabla^2 \Psi(\mathbf{x}) + \frac{qQ}{4\pi} \frac{1}{|\mathbf{x}|} \Psi(\mathbf{x}) \\ & + (1-8)\left(\frac{qQ}{4\pi}\right)^2 \frac{1}{4M} \frac{1}{|\mathbf{x}|^2} \Psi(\mathbf{x}). \end{aligned} \quad (3.2)$$

From (3.2) it follows that single photon exchange yields a repulsive potential term proportional to $(qQ)^2$ that decreases as the square of the distance between the constituents while the “seagull” interaction yields an attractive potential with the same form that is eight times as strong. To better compare the solutions here with those of Spence and Vary [7], in the nonrelativistic limit the potential term proportional to $(qQ)^2$ will be neglected. However, the effects of this term will be significant when (2.13), the Bethe-Salpeter equation in the instantaneous approximation, is solved in the next section.

To solve (3.1) a dimensionless momentum \mathbf{p}' is defined by

$$\mathbf{p}' \equiv \frac{\mathbf{p}}{\sqrt{-2\mu E'}}, \quad (3.3)$$

where μ is the reduced mass, $\mu = Mm/(M+m)$. Omitting the term proportional to $(qQ)^2$, (3.1) becomes

$$(1 + \mathbf{p}'^2) \Psi(\mathbf{p}') = \frac{qQ}{4\pi} \frac{\sqrt{-2\mu E'}}{2\pi^2 E'} \int_{-\infty}^{\infty} \frac{d^3 q'}{(\mathbf{p}' - \mathbf{q}')^2} \Psi(\mathbf{q}'). \quad (3.4)$$

Eq. (3.4) is the integral form of the Schrödinger equation for a quanta with mass μ and charge q interacting with a stationary charge Q via the Coulomb potential. Since the momentum variables are all now dimensionless, for notational convenience the primes will be omitted in future equations.

The solution is of the form

$$\Psi(\mathbf{p}) = R(p)Y_\ell(\theta, \phi). \quad (3.5)$$

Using Hecke’s theorem [18,19,20,10] the angular integration is easily performed. The angular dependence separates, yielding an integral equation,

$$(1 + p^2)pR(p) = \frac{qQ}{4\pi} \frac{\sqrt{-2\mu E'}}{\pi E'} \int_0^\infty dq Q_\ell\left(\frac{p^2 + q^2}{2pq}\right) qR(q). \quad (3.6)$$

Defining

$$\lambda \equiv \frac{qQ}{4\pi} \sqrt{\frac{-\mu}{2E'}}, \quad (3.7)$$

(3.6) becomes

$$(1 + p^2)pR(p) = \lambda \frac{2}{\pi} \int_0^\infty dq Q_\ell\left(\frac{p^2 + q^2}{2pq}\right) qR(q). \quad (3.8)$$

Theoretically,

$$\lambda = \ell + n; \quad n = 1, 2, \dots \quad (3.9)$$

Eq. (3.8) would be straightforward to solve numerically were it not for the fact that $Q_\ell((p^2 + q^2)/2pq)$ has a logarithmic singularity at $p = q$.

The boundary conditions are determined with the aid of the asymptotic relationship for Legendre functions of the second kind [21],

$$Q_\ell(z) \xrightarrow[z \rightarrow \infty]{} \frac{\sqrt{\pi} \Gamma(\ell + 1)}{2^{\ell+1} \Gamma(\ell + \frac{3}{2})} \frac{1}{z^{\ell+1}}. \quad (3.10)$$

At small p the function $pR(p)$ is assumed to be of the form

$$pR(p) \xrightarrow[p \rightarrow 0]{} p^{c_0} \quad (3.11)$$

where c_0 is a constant. From (3.10) it follows that at small p , $Q_\ell((p^2 + q^2)/2pq) \rightarrow p^{\ell+1}$. Equating the left- and right-hand sides of (3.7), at small p the equality $pR(p) \sim p^{\ell+1}$ is obtained, implying

$$c_0 = \ell + 1. \quad (3.12)$$

At large p the function $pR(p)$ is assumed to be of the form

$$pR(p) \xrightarrow[p \rightarrow \infty]{} \frac{1}{p^{c_\infty}}. \quad (3.13)$$

Using logic analogous to that which lead to (3.12),

$$c_\infty = \ell + 3. \quad (3.14)$$

Solutions are obtained by expanding $pR(p)$ in terms of N cubic B-splines $B_j(p)$ [8],

$$pR(p) = F(p) \sum_{j=1}^N c_j B_j(p). \quad (3.15)$$

By choosing the convergence function $F(p)$ in (3.15) so that at small and large p it behaves as the solution $pR(p)$ itself, fewer B-splines are required to represent solutions that go to zero rapidly at the boundaries.

Cubic B-splines are defined on five consecutive knots. To determine the spacing of the knots, $N-4$ zeros x_i of a Chebychev polynomial are calculated using the formula

$$x_i = -\cos \frac{(2i-1)\pi}{2(N-4)}, \quad i = 1, 2, \dots, N-4, \quad (3.16)$$

and then the knots T_{i+4} on the positive p -axis are determined by

$$T_{i+4} = C_1 \sqrt{\frac{1+x_i}{1-x_i}} + C_2, \quad i = 1, 2, \dots, N-4, \quad (3.17)$$

where C_1 and C_2 are constants. The knot T_4 is placed at the origin and three knots are placed on the “negative” p -axis to create maximum freedom in constructing the solution $pR(p)$ near the origin. The three knots on the “negative” p -axis are mirror images of the first three knots in (3.17).

Spence and Vary [7] note that integrals of the form

$$\int_0^\infty dp p^{\ell+k} Q_\ell \left(\frac{p^2 + q^2}{2pq} \right), \quad k = 0, 1, 2, \dots \quad (3.18)$$

are both finite and readily calculated analytically, so they choose $F(p)$ in (3.15) to be given by $F(p) = p^{\ell+1}$, which, from (3.12), automatically satisfies the boundary condition near $p = 0$ provided that the sum of B-splines in (3.15) are non-zero and slowly changing near the origin. Since the B-splines vanish at the largest knot, an appropriate sum of B-splines will satisfy the boundary condition at large p . However, the boundary conditions are satisfied both at small and at large p with the choice

$$F(p) = \frac{p^{\ell+1}}{(c^2 + p^2)^{\ell+\frac{3}{2}}} \quad (3.19)$$

where c is a constant. Note that at small p , $F(p) \rightarrow p^{\ell+1}$ as expected from (3.12), while at large p , $F(p) \rightarrow p^{-(\ell+2)}$, which is one power of p less than is indicated in (3.14). Since the last B-spline in the expansion (3.15) vanishes at the largest knot, the boundary conditions will be satisfied automatically both for small and large momenta provided that the sum of B-splines in (3.15) is slowly changing at small momenta and goes to zero as the reciprocal of the momentum at large momenta. By choosing $F(p)$ in (3.15) appropriately, solutions that decrease rapidly at small and large momenta can be accurately reproduced with fewer B-splines than when $F(p)$ is omitted.

Eq. (3.8) is solved numerically by converting the integral eigenvalue equation into a generalized matrix equation using the Rayleigh-Ritz-Galerkin method [21]. The solution is expanded in terms of B-splines using (3.15), and then both sides of (3.8) are multiplied by $B_i(p)F(p)$ and integrated over p . A generalized matrix equation results that is of the form $Ac = \lambda Bc$ where the matrices A and B are given, respectively, by

$$A_{ij} = \int_0^\infty dp B_i(p)F(p)(1+p^2)F(p)B_j(p) \quad (3.20a)$$

and

$$B_{ij} = \frac{2}{\pi} \int_0^\infty dp B_i(p)F(p) \int_0^\infty dq Q_\ell\left(\frac{p^2 + q^2}{2pq}\right)F(q)B_j(q). \quad (3.20b)$$

The elements of the column vector c are the expansion coefficients c_j in (3.15). Since both of the above matrices are symmetric and A_{ij} is positive definite, the eigenvalues are real [16].

The choice $F(p) = p^{\ell+1}$ works well for small values of angular momentum because the sum of a small number of B-splines readily creates a function that decreases as $p^{-(2\ell+4)}$ at large p , thus satisfying the boundary condition as given in (3.14). In addition, when $F(p) = p^{\ell+1}$, the integrals over $Q_\ell((p^2 + q^2)/2pq)$ in (3.20b) can be performed analytically because they are of the form (3.18). For larger values of angular momentum, however, the choice $F(p) = p^{\ell+1}$ does not work well because the sum of a small number of B-splines does not readily create a function that decreases sufficiently rapidly at large momentum so as to satisfy the boundary conditions.

The choice (3.19) for the convergence function immediately allows the boundary conditions to be satisfied by a sum of B-splines that is slowly changing, but now the integrals over q in (3.20b) can no longer be readily performed

analytically. The method for integrating the variable q over the singularity in the integrals is simple conceptually but somewhat involved numerically: Except in an ϵ -neighborhood of the singularity, all integrations are performed numerically using Gaussian quadrature with a seven-point option. As the integration variable approaches the singularity, where the integrand changes most rapidly, integration intervals are decreased to maintain accuracy of the numerical integration. Within an ϵ -neighborhood of the singularity, the integrand, excluding the associated Legendre function $Q_\ell((p^2 + q^2)/2pq)$, is expanded in a Taylor series about the singularity. The integral is then a sum of integrals of the form (3.18) that can be integrated analytically. The parameter ϵ is chosen to be the smaller of 0.01 or the distance from the singularity to the nearest knot, thus avoiding the complication of integrating over a knot.

To obtain a numerical estimate of the accuracy of each solution, the left- and right-hand sides of (3.6) are calculated midway between each pair of knots on the (positive) p -axis. A reliability coefficient R [14], which is a statistical measure of how closely the two sides of the equation agree at the selected points, is calculated. If the two sides of the equation agree exactly at all of the selected points, then R equals unity. Determining where the left- and right-hand sides of the equation agree least well reveals possible problems with trial solutions.

When $F(p) = p^{\ell+1}$, excellent solutions are obtained for $\ell = 0$ and $\ell = 1$. With 21 splines in the expansion (3.15), eigenvalues were obtained with four or five significant figures, and corresponding R -values were in the range $0.999 < R < 1.00$. However, when $\ell = 2$ as shown in second and third columns of Table 3.1, an incorrect eigenvalue appears with a corresponding $R = 0.00112$. For $\ell = 3$, the first few eigenvalues are accurate, but the corresponding R -values are on the order of 10^{-3} , indicating the solutions are unreliable. Examination of these solutions reveals that they are incorrect at large p . By choosing the convergence factor $F(p)$ as given in (3.18), the difficulties that appeared for $\ell > 1$ are eliminated as can be seen from the fourth and fifth columns of Table 3.1.

Table 3.1: Numerical values of $\lambda = \ell + 1, \ell + 2, \dots$ when 21 splines are used in the expansion (3.15).

	$F(p) = p^{\ell+1}$		$F(p) = p^{\ell+1}/\text{over}(c^2 + p^2)^{\ell+3/2}$	
ℓ	λ	R	λ	R
2	3.00000	0.99884	3.00000	1.0000
	4.00007	0.97013	4.00001	1.0000
	4.49547	0.00112	5.00003	1.0000
	5.00030	0.84320	6.00008	1.0000
3	4.00118	0.00266	4.00000	1.0000
	5.00844	-0.00028	5.00000	1.0000
	6.02762	-0.00031	6.00004	1.0000
	7.06566	-0.00023	6.99999	1.0000

4 Solutions of the Bethe-Salpeter Equation in the Instantaneous Approximation

Solutions to the Bethe-Salpeter equation in the instantaneous approximation are obtained using two different basis systems. The first basis system is comprised of essentially the same basis functions that were employed to calculate solutions to the nonrelativistic hydrogen atom. Because the basis functions vanish at large momenta, they are particularly suitable for representing solutions that have significant support only to moderately large values of momentum (and position). For this basis system four B-splines are non-zero between consecutive knots in the physical region except for the final four knots at the largest values of momentum: There the number of non-zero B-splines between consecutive knots decreases from three to two until only one B-spline is non-zero between the final two knots, thus making it increasingly difficult to express a solution at large momentum in terms of these basis functions. To better represent solutions that are highly localized in position space and, therefore, have significant support at large values of momentum, a second basis system is used in which some basis functions vanish only at infinite values of momentum and four B-splines are non-zero between consecutive knots in the physical region.

The boundary conditions as p approaches zero and infinity are determined using the same procedure employed in the previous section. The results are as follows:

$$pG(p) \xrightarrow[p \rightarrow 0]{} p^{j+\frac{1}{2}} \quad pF(p) \xrightarrow[p \rightarrow 0]{} p^{j+\frac{3}{2}} \quad (4.1a)$$

$$pG(p) \xrightarrow[p \rightarrow \infty]{} \frac{1}{p^{j+\frac{3}{2}}} \quad pF(p) \xrightarrow[p \rightarrow \infty]{} \frac{1}{p^{j+\frac{5}{2}}} \quad (4.1b)$$

Solutions can be obtained using methods of the previous section and are of the form

$$pG(p) = \mathcal{G}_1(p) \sum_{j=1}^N g_j B_j(p), \quad (4.2a)$$

and

$$pG(p) = \mathcal{F}_1(p) \sum_{j=1}^N f_j B_j(p). \quad (4.2b)$$

The convergence functions $\mathcal{G}_1(p)$ and $\mathcal{F}_1(p)$ are chosen so that the boundary conditions are automatically satisfied provided that the sums of B-splines in the previous equation are slowly changing for small and large momenta.

$$\mathcal{G}_1(p) = \frac{p^{j+\frac{1}{2}}}{(c_{\mathcal{G}}^2 + p^2)^{j+\frac{1}{2}}} \quad \mathcal{F}_1(p) = \frac{p^{j+\frac{3}{2}}}{(c_{\mathcal{F}}^2 + p^2)^{j+\frac{3}{2}}} \quad (4.3)$$

In the above equation $c_{\mathcal{G}}$ and $c_{\mathcal{F}}$ are constants. Note that at small p , $p\mathcal{G}_1(p)$ and $p\mathcal{F}_1(p)$ vanish as indicated in (4.1a), but at large p they decrease by a factor p more slowly than indicated in (4.1b) because the B-splines themselves vanish at large p . As can be seen from (4.3), solutions go to zero rapidly at the boundaries even at the smallest value $j = 1/2$, so it would be difficult to obtain any accurate solutions in the instantaneous approximation without using convergence functions.

Eq. (2.21) is converted into a generalized matrix equation of the form

$$A \begin{bmatrix} g \\ f \end{bmatrix} = \epsilon B \begin{bmatrix} g \\ f \end{bmatrix} \quad (4.4)$$

by multiplying the top and bottom equations by $\mathcal{G}_1(p)B_i(p)$ and $\mathcal{F}_1(p)B_i(p)$, respectively, and then integrating over p . The elements of the column vectors g and f are, respectively, the expansion coefficients g_j and f_j in (4.2). Since the matrices A and B have been constructed so that both are symmetric and B is positive definite, the dimensionless energy eigenvalue ϵ is forced to be real [16] as required.

The Bethe-Salpeter equation in the instantaneous approximation contains double integrals while in the nonrelativistic limit, the equation involves only single integrals. In spite of this complication, by performing integrations in a specific order, all integrals with a logarithmic singularity that are necessary to solve the equation are of the form already encountered in the previous section. However, the technique used to integrate over the logarithmic singularity in the previous section fails at very large values of momentum: All of the terms being expanded in a Taylor series about the singular point p are functions of q^2 with the result that a typical term in the expansion is $a_n(q^2 - p^2)^n$. Within an ϵ -neighborhood of p , the maximum value of $q^2 - p^2$ is $2p\epsilon$. When p is of the order of $1/\epsilon$ the expansion begins to lose accuracy. By choosing ϵ to decrease linearly with increasing p , this problem is avoided.

To check the accuracy of the solutions by calculating the reliability coefficient, double integrals of the following form must be evaluated:

$$\int_0^\infty \frac{dq}{\omega_-(q)} Q_\ell\left(\frac{p^2 + q^2}{2pq}\right) \int_0^\infty dk Q_\ell\left(\frac{k^2 + q^2}{2kq}\right) \frac{q^{\ell+d_1}}{(c^2 + k^2)^{d_2}} B_j(k) \quad (4.5)$$

The integral over the variable k can be calculated as previously discussed. Except within an ϵ -neighborhood of the logarithmic singularity of the integrand, the integral over the variable q is evaluated numerically. Within the ϵ -neighborhood, the integral over k is expressed as a power series expansion in the variable q ,

$$\int_0^\infty dk Q_\ell\left(\frac{k^2 + q^2}{2kq}\right) \frac{q^{\ell+d_1}}{(c^2 + k^2)^{d_2}} B_j(k) = q^{\ell+1} \sum_{j=0}^3 a_j (q - p)^j. \quad (4.6)$$

The power series expansion in the above equation depends on the fact that the integral vanishes as $q^{\ell+1}$ at small q , a fact that is readily verified using (3.10). The coefficients a_j are determined numerically so that the expansion and the integral agree at $p + \epsilon$, $p + \epsilon/3$, $p - \epsilon/3$ and $p - \epsilon$. Using the expansion in (4.6), within the ϵ -neighborhood of the logarithmic singularity at p , the integral (4.5) can be performed analytically.

To better represent solutions that are highly localized in position space and, therefore, have significant support at large values of momentum, a second basis system is introduced in which some basis functions vanish only at infinity. To construct the basis system, the momentum is first mapped onto

a compact space with the transformation

$$x(p) = b \frac{p^2 - a}{p^2 + a}, \quad (4.7)$$

where a and b are constants. From (4.7) it follows that $-b \leq x(p) \leq b$.

The knots are determined by first calculating $N - 8$ zeros x_i of a Chebychev polynomial using the formula

$$x_i = -\cos \frac{(2i - 1)\pi}{2(N - 8)}, \quad i = 1, 2, \dots, N - 8. \quad (4.8)$$

The knots in the region $-b < x < b$ are then given by

$$T_{i+4} = bx_i, \quad i = 1, 2, \dots, N - 8. \quad (4.9)$$

The knot T_4 is placed at $x = -b$ ($p = 0$) and three knots are placed in the region $x < -b$ (on the “negative” p -axis) to create maximum freedom in constructing solutions near the origin. The three knots in the region $x < -b$ are mirror images of the first three knots in (4.9). In a similar fashion the knot T_{N-3} is placed at $x = b$ ($p = \infty$) and three knots are placed in the region $x > b$ (“ $p > \infty$ ”) to create maximum freedom in constructing solutions at very large momenta. The three knots in the region $x > b$ are mirror images of the final three knots in (4.9). With the above knot structure, four B-splines are non-zero between each pair of adjacent knots in the entire physical region $0 \leq p \leq \infty$.

The solution is expanded in terms of B-splines as follows:

$$pG(p) = \mathcal{G}_2(p(x)) \sum_{j=1}^N g_j B_j(x), \quad (4.10a)$$

and

$$pG(p) = \mathcal{F}_2(p(x)) \sum_{j=1}^N f_j B_j(x), \quad (4.10b)$$

where

$$\mathcal{G}_2(p) = \frac{p^{j+\frac{1}{2}}}{(c_{\mathcal{G}}^2 + p^2)^{j+1}}, \quad \mathcal{F}_2(p) = \frac{p^{j+\frac{3}{2}}}{(c_{\mathcal{F}}^2 + p^2)^{j+2}}. \quad (4.11)$$

For the second basis system the final three B-splines in the expansion are non-zero at $x = b$ ($p = \infty$). Consequently, solutions that have significant support at large values of momentum are more readily expressed in terms of the second set of basis functions. Since some B-splines are finite at $p = \infty$, the functions $\mathcal{G}_2(p)$ and $\mathcal{F}_2(p)$ are chosen to satisfy the boundary conditions (4.1) both at small and large momenta.

To integrate over singularities at large values of momentum p , the integrand is expanded in a Maclaurin series in the variable $1/q$ instead of in a Taylor series. Specifically, if the location of the first knot less than the singularity corresponds to a value of momentum equal to or less than 50, then integrals are evaluated as previously discussed. On the other hand, if the first knot less than the singularity corresponds to a value of momentum greater than 50, the integral is evaluated numerically from $x = -b$ ($p = 0$) to the knot. From the knot to $x = b$ ($p = \infty$), the integral is evaluated analytically by expanding the integrand, excluding the Legendre function of the second kind, in a Maclaurin series. The necessary formulas for carrying out the integration are given in the appendix.

A corresponding modification is required to evaluate the double integrals (4.5). When the location of first knot less than the logarithmic singularity at $q = p$ corresponds to a value of p equal to or less than 50, the integral is evaluated as before. When the position of the knot corresponds to a value of p greater than than 50, the integral is evaluated numerically except within an ϵ -neighborhood of the singularity by expanding the integral over k as a Maclaurin series in the variable $1/q$,

$$\int_0^\infty dk \ Q_\ell\left(\frac{k^2 + q^2}{2kq}\right) \frac{q^{\ell+d_1}}{(c^2 + k^2)^{d_2}} B_j(k) = \frac{1}{q^{\ell+1}} \sum_{j=0}^3 a_j \frac{1}{q^j}. \quad (4.12)$$

In writing the expansion, the fact has been used that the integral vanishes as $1/q^{\ell+1}$ at large q . The coefficients a_j are determined numerically so that the expansion and the integral agree at $p + \epsilon$, $p + \epsilon/3$, $p - \epsilon/3$ and $p - \epsilon$. Using the expansion in (4.12), within the ϵ -neighborhood of the logarithmic singularity at p , the integral (4.5) can be performed analytically.

The first basis system has more knots concentrated at small values of momentum and, therefore, is more suitable for representing weakly-bound solutions or solutions with detailed structure in this region. The second basis system has more knots at large values of momentum and is better for

representing strongly-bound solutions that have significant support at large values of momentum. However, at least when 35 or fewer splines are used, the second basis system does not adequately represent the most strongly bound solutions with ϵ on the order of or less than about 0.3. Of course, for such states the instantaneous approximation is not a satisfactory approximation to the Bethe-Salpeter equation.

When only the effects of single-photon exchange are included, the solutions in the instantaneous approximation are approximate solutions of the Bethe-Salpeter equation in the ladder approximation. If the masses of the constituents are equal, zero-energy, analytical solutions exist for the Bethe-Salpeter equation in the ladder approximation for several values of $qQ/4\pi$ in the range $0 < qQ/4\pi < 100$ [10]. In the instantaneous approximation, when only single-photon exchange is included, no bound-state solutions were found with either zero or finite energy within this range of coupling constants.

For all data graphed below, the constituent masses are equal although solutions with unequal constituent masses are no more difficult to determine. Solutions were calculated using the two different basis systems previously discussed. For values of $\epsilon = E/(M + m) > 0.95$, the graphed results are those obtained from the first basis system, which has more knots at small momenta. For all other values of ϵ , the graphs are an average of the solutions obtained from the two basis systems. Solutions for ϵ obtained from the two different basis systems almost always agreed within 0.04 and usually agreed more closely while reliability coefficients were almost always greater than 0.99. Solutions were calculated by expanding the wave function in terms of 35 B-splines.

From Fig. 4.1, as the coupling constant decreases in magnitude, the repulsive effects of angular momentum become apparent so that states with higher angular momentum are more weakly bound.

Because the bound states in Fig. 4.2 include the “seagull” term, for the same value of the coupling constant these states are significantly more tightly bound than the corresponding states in Fig. 4.1, which only include single-photon exchange.

The bound states in Fig. 4.3 that occur for positive values of $qQ/4\pi$ are the result of the “seagull” interaction, which is always attractive nonrelativistically. As a consequence, like-signed electric charges can attract [10]. But, at least for equal-mass constituents in the instantaneous approximation as shown in Fig. 4.3(a), no binding occurs between like-signed charges for

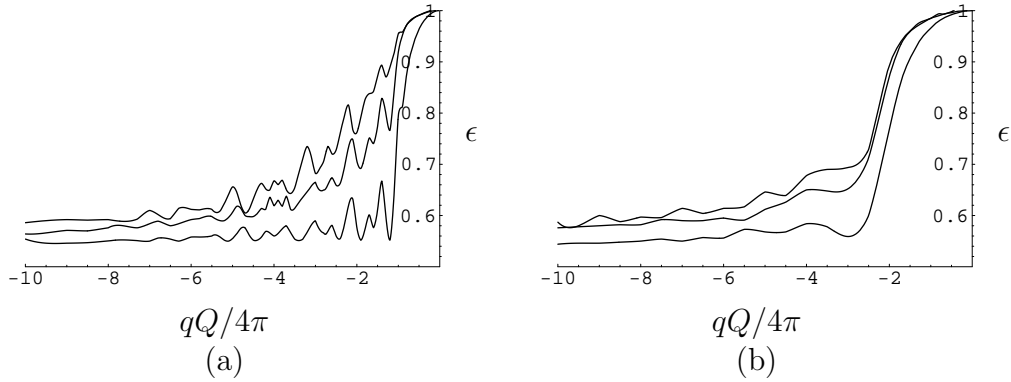


Figure 4.1: The dimensionless energy eigenvalues $\epsilon = E/(M + m)$ of the three lowest bound states as a function of the coupling constant $qQ/4\pi$ when only single-photon exchange is included in the instantaneous approximation. Graphs (a) and (b) correspond to angular momentum $j = 1/2$ and $j = 3/2$, respectively.

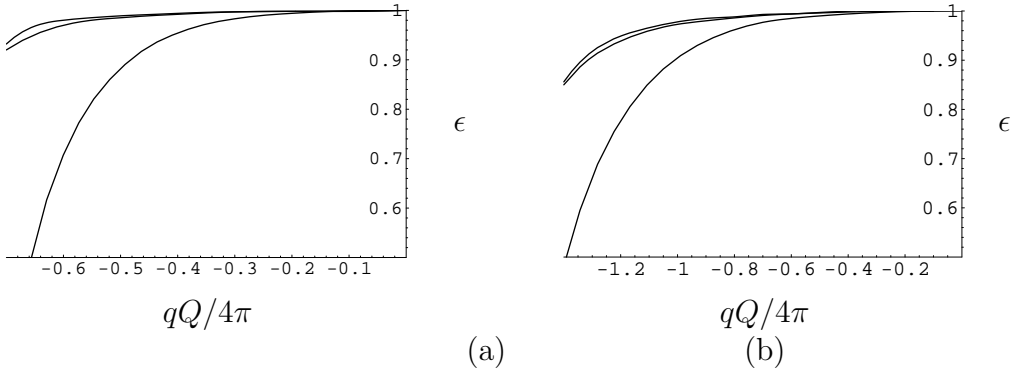


Figure 4.2: The dimensionless energy eigenvalues $\epsilon = E/(M + m)$ of the three lowest bound states as a function of the coupling constant $qQ/4\pi$ in the instantaneous approximation. Graphs (a) and (b) correspond to angular momentum $j = 1/2$ and $j = 3/2$, respectively.

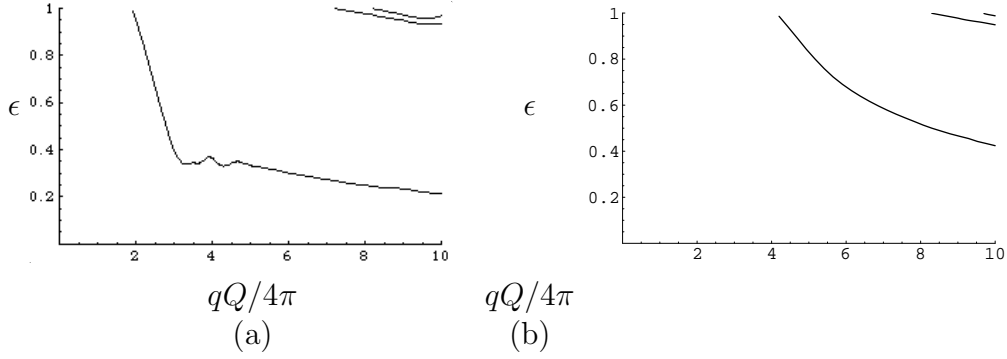


Figure 4.3: The dimensionless energy eigenvalues $\epsilon = E/(M + m)$ of the three lowest bound states as a function of the coupling constant $qQ/4\pi$ in the instantaneous approximation. Graphs (a) and (b) correspond to angular momentum $j = 1/2$ and $j = 3/2$, respectively.

values of $qQ/4\pi < 1.9$. Since no “elementary” constituent could have such a large charge, the effect would not be observable. On the other hand, by considering the fully relativistic equation with unequal-mass constituents, if such binding could be achieved for constituents that have charges with magnitudes on the order of e , the effect might be observable.

5 Conclusions

In spite of a derivative coupling in the Lagrangian, the Bethe-Salpeter equation, which includes the effects of both single-photon exchange and the “seagull” interaction, can readily be solved in the instantaneous approximation: Terms appear symmetrically in the equation so that it can be converted to a generalized matrix eigenvalue equation of the form $Ac = \epsilon Bc$ where the matrices A and B are symmetric and B is positive definite, a sufficient condition for yielding real eigenvalues ϵ . Using a generalization of a method introduced by Spence and Vary [7] for handling logarithmic singularities in integrands, basis systems are used that automatically satisfy the boundary conditions, making it possible to obtain solutions in the instantaneous approximation. Weakly-bound solutions are more efficiently obtained by writing the solution in terms of basis functions that extend only to finite values of momentum while solutions with large binding energies are obtained

more accurately by mapping the momentum onto a compact space and then expressing the solutions in terms of basis functions, some of which vanish only at infinity. A statistical measure is used to provide an indication of the accuracy of solutions by determining how well the wave functions satisfy the equation midway between each knot in the physical region.

Acknowledgments

I would like to thank Professor John J. Skowronski for very helpful discussions regarding statistical parameters that would indicate the reliability of numerical solutions to equations. Dr. David G. Robertson assisted in optimizing the code. This work was supported by a grant of computer time from the Ohio Supercomputer Center.

Appendix: Calculation of Integrals

Here the formulas are given for calculating the integrals of the form

$$B_{(a,b)}^{\ell,k}(p) \equiv \int_a^b dq Q_\ell\left(\frac{p^2 + q^2}{2pq}\right) \frac{1}{q^{\ell+k}} \quad \begin{aligned} \ell &= 0; & k &= 1, 2, 3, \dots \\ \ell &\geq 1; & k &= 0, 1, 2, \dots \end{aligned} \quad (A1)$$

that are required to integrate over the logarithmic singularities when they occur at large p . Using the recursion formula for Legendre functions of the second kind [23],

$$Q_{\ell+1}(z) = \frac{2\ell+1}{\ell+1} z Q_\ell(z) - \frac{\ell}{\ell+1} Q_{\ell+1}(z), \quad (A2)$$

a recursion relation for $B_{(a,b)}^{\ell,k}(p)$ follows immediately:

$$B_{(a,b)}^{\ell+1,k}(p) = \frac{2\ell+1}{\ell+1} \left[\frac{p}{2} B_{(a,b)}^{\ell,k+2}(p) + \frac{1}{2p} B_{(a,b)}^{\ell,k}(p) \right] - \frac{\ell}{\ell+1} B_{(a,b)}^{\ell-1,k+2}(p) \quad (A3)$$

The integrals $B_{(a,b)}^{\ell,k}(p)$ are readily expressed in terms of the integrals

$$I_{(a,b)}^k(p) \equiv \int_a^b dq \frac{\ln(q+p)}{q^k}. \quad (A4)$$

Specifically,

$$B_{(a,b)}^{0,k}(p) = I_{(a,b)}^k(p) - I_{(a,b)}^k(-p) \quad (A5)$$

and

$$\begin{aligned} B_{(a,b)}^{1,k}(p) &= \frac{p}{2}[I_{(a,b)}^{k+2}(p) - I_{(a,b)}^{k+2}(-p)] + \frac{1}{2p}[I_{(a,b)}^k(p) - I_{(a,b)}^k(-p)] \\ &+ \left\{ \begin{array}{ll} -\ln\left(\frac{b}{a}\right) & \text{if } k = 0 \\ \frac{1}{k}\left[\frac{1}{b^k} - \frac{1}{a^k}\right] & \text{if } k > 0 \end{array} \right\}. \end{aligned} \quad (A6)$$

The integrals $I_{(a,b)}^0(p)$ and $I_{(a,b)}^1(p)$ are calculated using standard tables of integrals [23], although $I_{(a,b)}^1(p)$ is evaluated as an infinite series. For $k \geq 2$, the integral $I_{(a,b)}^k(p)$ can be calculated using the following formula: Let

$$I \equiv \int dx \frac{\ln(a+bx)}{x^k}, \quad k \geq 2. \quad (A7)$$

Integrating by parts,

$$I = \frac{1}{k-1} \left[-\frac{\ln(a+bx)}{x^{k-1}} + b \int \frac{dx}{x^{k-1}(a+bx)} \right].$$

The integral in the above expression is evaluated using partial fractions, yielding the desired formula:

$$\begin{aligned} I &= \frac{1}{k-1} \left[-\frac{\ln(a+bx)}{x^{k-1}} + \left(-\frac{b}{a}\right)^{k-1} \ln(a+bx) \right. \\ &\quad \left. - \left(-\frac{b}{a}\right)^{k-1} \ln(x) + \sum_{j=2}^{k-1} \left(-\frac{b}{a}\right)^{k-j} \frac{1}{(j-1)x^{j-1}} \right] \end{aligned} \quad (A8)$$

References

1. E.E. Salpeter and H.A. Bethe, Phys. Rev. **84**, 1232 (1951).
2. G.B. Mainland, Few Body Systems **26**, 27 (1999).
3. R. Blankenbecler and R. Sugar, Phys. Rev. **142**, 1051 (1966).
4. E.E. Salpeter, Phys. Rev. **87**, 328 (1952).
5. J.L. Gammel and M.T. Menzel, Phys. Rev. **A7**, 858 (1973).
6. D. Eyre and J.P. Vary, Phys. Rev. **D34**, 3467 (1986).
7. J.R. Spence and J.P. Vary, Phys. Rev. **D35**, 2191 (1987); Phys. Rev. **C47**, 1282 (1993).
8. See, for example, C. de Boor, *A Practical Guide to Splines* (Springer-Verlag, Berlin-Heidelberg-New York, 1978).
9. J.C. Pati and A. Salam, Phys. Rev. **D10**, 275 (1974); J.C. Pati, A. Salam and J. Strathdee, Phys. Lett. **B59**, 265 (1975); O.W. Greenberg and J. Sucher, Phys. Lett. **B99**, 339 (1981); W. Buchmuller, R.D. Pecci and T. Yanagida, Phys Lett. **B124**, 67 (1983); O.W. Greenberg, R.N. Mohapatra and M. Yasue, Phys. Rev. Lett. **51**, 1737 (1983); Nucl. Phys. **B237**, 189 (1984); J.C. Pati, Phys. Rev. **D30**, 1144 (1984) M.A. Luty and R.N. Mohapatra, Phys. Lett. **B 396**, 161 (1997).
10. G.B. Mainland, J. Math. Phys. **27**, 1344 (1986).
11. S. Godfrey and N. Isugur, Phys. Rev. **D32**, 189 (1985); S. Godfrey, Nuovo Cimento **A102**, 1 (1989); W. Lucha, F.F. Schöberl and D. Gromes, Phys. Rep. **200**, 127 (1991); A.J. Sommerer, J.R. Spence and J.P. vary, Phys. Rev. **C49**, 513 (1994).
12. S. Hatakeyama *et al*, Phys. Rev. Lett. **81**, 2016 (1998).
13. N. Arkani-Hamed and Y. Grossman, Phys. Lett. **B 459**, 179 (1999).
14. B.J. Winer, *Statistical Principles in Experimental Design* (McGraw Hill, New York, 1962).

15. The notation is that of J.D. Bjorken and S.D. Drell, *Relativistic Quantum Fields* (McGraw Hill, New York, 1965). \hbar and c are set to unity. Repeated Greek indices are summed from 0-3 and repeated Roman indices are summed from 1-3. Bold variables represent vectors in three-dimensional space.
16. See, for example, F.B. Hildebrand, *Methods of Applied Mathematics*, 2nd Ed. (Prentice-Hall, Englewood Cliffs, New Jersey, 1965).
17. C. Schwartz, Phys. Rev. **137**, B717 (1965); M.J. Zuilhof and J.A. Tjon, Phys. Rev. **C22**, 2369 (1980); G. B. Mainland and J.R. Spence, Few Body Systems **19**, 109 (1995); T. Nieuwenhuis and J.A. Tjon, Few Body Systems **21**, 167 (1996).
18. E. Hecke, Math. Ann. **78**, 398 (1918).
19. V. Fock, Z. Phys. **98**, 145 (1935).
20. M. Le  y, Proc. R. Soc. London Ser. **A204**, 145 (1950).
21. P.M. Morse and H. Feshbach, *Methods of Theoretical Physics* (McGraw-Hill, New York, 1953).
22. K.E. Atkinson, *A Survey of Numerical Methods for the Solution of Fredholm Equations of the Second Kind* (SIAM, Philadelphia, 1976); L.M. Delves and J. Walsh, *Numerical Solution of Integral Equations* (Clarendon Press, Oxford, 1974).
23. I.S. Gradshteyn and I.M. Ryzhik *Tables of Integrals, Series, and Products* (Academic Press, New York, 1965).